A multi-functional plasmonic biosensor

Yun-Tzu Chang[1], Yueh-Chun Lai[1], Chung-Tien Li[1], Cheng-Kuang Chen[1], Ta-Jen Yen[1,2,3,*]

[1] *Department of Materials Science and Engineering, National Tsing Hua University, Hsinchu 30013, Taiwan, Republic of China*
[2] *Institute of NanoEngineering and MicroSystems, National Tsing Hua University, 101, Section 2, Kuang Fu Road, Hsinchu 30013, Taiwan, Republic of China*
[3] *Tel: 886-3-5742174; Fax: 886-3-5722366*
**tjyen@mx.nthu.edu.tw*

Abstract: We present a coupler-free, multi-mode refractive index sensor based on nanostructured split ring resonators (SRRs). The fabricated SRR structures exhibit multiple reflectance peaks, whose spectral positions are sensitive to local dielectric environment and can be quantitatively described by our standing-wave plasmonic resonance model, providing a design rule for this multi-mode refractive-index (MMRI) sensor. We further manifest that the lower-order modes possess greater sensitivity associated with stronger localized electromagnetic field leading to shorter detection lengths within five hundreds nanometers, while the higher-order modes present mediate sensitivity with micron-scale detection lengths to allow intracellular bio-events detection. These unique merits enable the SRR-based sensor a multi-functional biosensor and a potential label-free imaging device.

OCIS codes: (160.3918) Metamaterials; (260.5740) Resonance; (130.6010) Sensors.

References and links

1. J. Homola, S. S. Yee, and G. T. Gauglitz, "Surface plasmon resonance sensors: review," Sens. Act. B **54**(1-2), 3–15 (1999).
2. H. Raether, "Surface plasmons on smooth and rough surfaces and on gratings," Springer (1988).
3. V. G. Veselago, "The electrodynamics of substances with simultaneously negative values of ε and μ," Sov. Phys. Usp. **10**(4), 509–514 (1968).
4. J. B. Pendry, A. J. Holden, W. J. Stewart, and I. Youngs , "Extremely low frequency plasmons in metallic mesostructures," Phys. Rev. Lett. **76**(25), 4773–4776 (1996).
5. J. B. Pendry, A. J. Holden, D. J. Robbins, and W. J. Stewart, "Magnetism from conductors and enhanced nonlinear phenomena," IEEE Trans. Microw. Theory Tech. **47**(11), 2075–2084 (1999).
6. R. A. Shelby, D. R. Smith, and S. Schultz, "Experimental verification of a negative index of refraction," Science **292**(5514), 77–79 (2001).
7. J. B. Pendry, "Negative refraction makes a perfect lens," Phys. Rev. Lett. **85**(18), 3966–3969 (2000).
8. X. Zhang, and Z. Liu, "Superlenses to overcome the diffraction limit," Nat. Mater. **7**(6), 435–441 (2008).
9. D. Schurig, J. J. Mock, B. J. Justice, S. A. Cummer, J. B. Pendry, A. F. Starr, and D. R. Smith, "Metamaterial electromagnetic cloak at microwave frequencies," Science **314**(5801), 977–980 (2006).
10. J. B. Pendry, D. Schurig, and D. R. Smith, "Controlling electromagnetic fields," Science **312**(5781), 1780–1782 (2006).
11. M. I. Stockman, "Spasers explained," Nat. Photonics **2**(6), 327–329 (2008).
12. R. F. Oulton, V. J. Sorger, T. Zentgraf, R. M. Ma, C. Gladden, L. Dai, G. Bartal, and X. Zhang, "Plasmon lasers at deep subwavelength scale," Nature **461**(7264), 629–632 (2009).
13. T. J. Yen, W. J. Padilla, N. Fang, D. C. Vier, D. R. Smith, J. B. Pendry, D. N. Basov, and X. Zhang, "Terahertz magnetic response from artificial materials," Science **303**(5663), 1494–1496 (2004).
14. N. Katsarakis, T. Koschny, M. Kafesaki, E. N. Economou, and C. M. Soukoulis, "Electric coupling to the magnetic resonance of split ring resonators," Appl. Phys. Lett. **84**(15), 2943 (2004).
15. C. Rockstuhl, F. Lederer, C. Etrich, T. Zentgraf, J. Kuhl, and H. Giessen, "On the reinterpretation of resonances in split-ring-resonators at normal incidence," Opt. Express **14**(19), 8827–8836 (2006).
16. J. Zhou, T. Koschny, and C. M. Soukoulis, "Magnetic and electric excitations in split ring resonators," Opt. Express **15**(26), 17881–17890 (2007).
17. A. W. Clark, A. K. Sheridan, A. Glidle, D. R. S. Cumming, and J. M. Cooper, "Tunable visible resonances in crescent shaped nano-split-ring resonators," Appl. Phys. Lett. **91**(9), 093109 (2007).
18. C. Y. Chen, S. C. Wu, and T. J. Yen, "Experimental verification of standing-wave plasmonic resonances in split-ring resonators," Appl. Phys. Lett. **93**(3), 034110 (2008).

#125448 - $15.00 USD Received 19 Mar 2010; revised 14 Apr 2010; accepted 14 Apr 2010; published 22 Apr 2010

19. C. Y. Chen, and T. J. Yen, "Electric and magnetic responses in the multiple-split ring resonators by electric excitation," J. Appl. Phys. **105**(12), 124913 (2009).
20. T. Driscoll, G. O. Andreev, D. N. Basov, S. Palit, S. Y. Cho, N. M. Jokerst, and D. R. Smith, "Tuned permeability in terahertz split-ring resonators for devices and sensors," Appl. Phys. Lett. **91**(6), 062511 (2007).
21. Y. Sun, X. Xia, H. Feng, H. Yang, C. Gu, and L. Wang, "Modulated terahertz responses of split ring resonators by nanometer thick liquid layers," Appl. Phys. Lett. **92**(22), 221101 (2008).
22. S. Y. Chiam, R. Singh, J. Gu, J. Han, W. Zhang, and A. A. Bettiol, "Increased frequency shifts in high aspect ratio terahertz split ring resonators," Appl. Phys. Lett. **94**(6), 064102 (2009).
23. H. J. Lee, and J. G. Yook, "Biosensing using split-ring resonators at microwave regime," Appl. Phys. Lett. **92**(25), 254103 (2008).
24. C. Debus, and P. H. Bolivar, "Frequency selective surfaces for high sensitivity terahertz sensing," Appl. Phys. Lett. **91**(18), 184102 (2007).
25. J. F. O'Hara, R. Singh, I. Brener, E. Smirnova, J. Han, A. J. Taylor, and W. Zhang, "Thin-film sensing with planar terahertz metamaterials: sensitivity and limitations," Opt. Express **16**(3), 1786–1795 (2008).
26. A. Cunningham, "Introduction to Bioanalytical Sensors (techniques In Analytical Chemistry)," John Wiley & Sons (1998).
27. J. J. Mock, D. R. Smith, and S. Schultz, "Local Refractive Index Dependence of Plasmon Resonance Spectra from Individual Nanoparticles," Nano Lett. **3**(4), 485–491 (2003).
28. M. M. Miller, and A. A. Lazarides, "Sensitivity of metal nanoparticle plasmon resonance band position to the dielectric environment as observed in scattering," J. Opt. A, Pure Appl. Opt. **8**(4), 239 (2006).

The current prevailing technique of refractive index sensors for biological applications is surface plasmon resonance (SPR) owing to its label-free and sensitive nature [1]. Nevertheless, an SPR system demands optical couplers (e.g., prisms and gratings), displays narrow operation ranges (typically at visible frequencies) and performs short detection distances typically within a couple of hundreds of nanometers [2], thus impeding its integration with low-cost, real-time and high throughput biochips for rapid bio-analytical measurements of quantity-limited samples. To overcome these issues, here we present a split-ring resonator (SRR) based plasmonic sensor to substantially ease the burdens aforementioned (coupler free, tunable operation frequencies and longer detection length) and meanwhile to preserve the merit of the conventional SPR technique (excellent sensitivity, label free, quick and real-time diagnose). The SRR structures exhibit multiple reflectance peaks, whose spectral positions are sensitive to local dielectric environment and can be quantitatively described by our standing-wave plasmonic resonance model, providing a design rule for this multi-mode refractive-index (MMRI) sensor. We further manifest that the lower-order modes possess greater sensitivity associated with stronger localized electromagnetic field leading to shorter detection lengths within five hundreds nanometers, while the higher-order modes present mediate sensitivity with micron-scale detection lengths to allow intracellular bio-events detection. These merits enable the SRR-based sensor a multi-functional plasmonic biosensor and a potential label-free bioimaging device.

By substituting naturally existing atoms with artificially constructed meta-atoms, meta-materials own unprecedented electromagnetic properties [3–5] such as negative refraction [6], super-lensing effect [7, 8], cloaking of invisibility [9, 10], SPASER [11, 12] and more. Among diverse metamaterials, it is the split-ring resonator (SRR) structure a pioneering design proposed by Pendry et al. as magnetic meta-atoms to achieve negative magnetic permeability [5] and high-frequency magnetism [13]. Ever since then, SRRs have increasingly attracted great attentions and recent efforts were thrown into investigating their fundamental electromagnetic responses [14–17] and potential applications. Until today, the veiled physics of SRRs has become much clearer, for example, the multiple resonant reflectance peaks under normal incidence can be interpreted by model of standing-wave plasmonic resonances [18, 19]. More importantly, such a resonance condition depends on the local dielectric environment so sensitively that the SRRs can be readily employed as refractive-index (RI) sensors [20], especially for real-time, label-free and cell-level bimolecular detections by monitoring the shifts of reflectance peaks as analytes binding to molecular receptors immobilized on the SRR surface.

Recently, the sensing possibility and capability of the planar SRR structure have been reported [21–25], but it still lacks a comprehensive understanding of the relative sensitivity and the detection length about the multi-mode plasmonic resonances in the planar SRR structure. As a consequence, by applying thin dielectric layers with different thicknesses on the SRR array, we demonstrate a quantitative interpretation to the distinct sensing behaviors (including sensitivity and detection length) of each resonance mode in the multi-resonance reflectance spectra based on both simulation and experimental results, present a coupler-free, scalable and multi-mode refractive index sensor based on nano-structured split ring resonators (SRRs). Figure 1(a) shows the design of the SRR unit cell specified by side length d, gap g, linewidth w and total length L = 4(d-w)-g, respectively. To reveal the influence of total length L on the resonance response, five different sized SRR square arrays were fabricated by 50 nm thick gold layers on transparent quartz substrates with an area of 100×100μm^2 through E-beam lithographic and lift-off processes as shown in Fig. 1(b). The details of the measured geometric parameters of each sample can be found in Table 1. Next, the fabricated SRRs were characterized by a micro-Fourier transform infrared spectroscopic system (μ-FTIR) in reflectance measurements directly under normal incidence without using optical couplers.

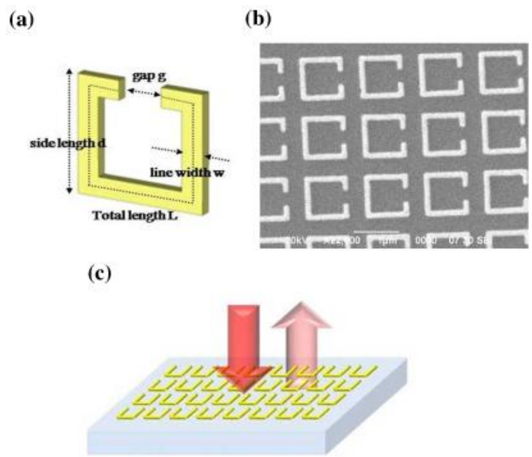

Fig. 1. (a) The designed SRR unit cell. (b) SEM images of fabricated planar SRRs. (c) Schematic reflectance measurement upon the SRR-based plasmonic sensor. Here no optical coupler is required to excite plasmonic resonance. The details of the measured geometric parameters of five samples can be found in supporting information.

Table 1. Measured geometrical parameters of the fabricated planar SRRs.

Design (nm)	Side length (nm)	Gap (nm)	Line width (nm)	Total length (nm)	Periodicity (nm)
d720	750	157	102	2435	1030
d600	640	210	106	1926	840
d510	532	170	98	1566	705
d450	485	145	99	1400	632
d300	360	140	75	1000	470

The measured spectra are shown in Fig. 2, presenting multiple reflectance peaks whose resonance wavelengths can be interpreted by the standing-wave plasmonic resonance (SWPR) model [18]:

$$L = \frac{m(\lambda_m + \lambda_0)}{2n_{eff}} \qquad (1)$$

where L denotes the total length of SRR, λ_m is the resonance wavelength, m is the resonance mode, n_{eff} is the effective refractive index of the dielectric environment and λ_0 depends on the

#125448 - $15.00 USD Received 19 Mar 2010; revised 14 Apr 2010; accepted 14 Apr 2010; published 22 Apr 2010

geometric structure. Notice the multiple reflectance peaks are denoted as two sets of resonance modes: $1_{\|}$, $3_{\|}$, $5_{\|}$, $7_{\|}$ and $2\perp$, $4\perp$, $6\perp$, $8\perp$ corresponding to two orthogonal E-filed polarization directions ($E_{\|}$ and $E\perp$), respectively. Next, we plot the resonance wavelengths (λ_m) versus the reciprocal of resonance mode (1/m) among different sized SRRs. As shown in Fig. 3, all curves show a clear linear relationship and among them, the longer SRR displays a greater slope that is consistent with the Eq. (1).

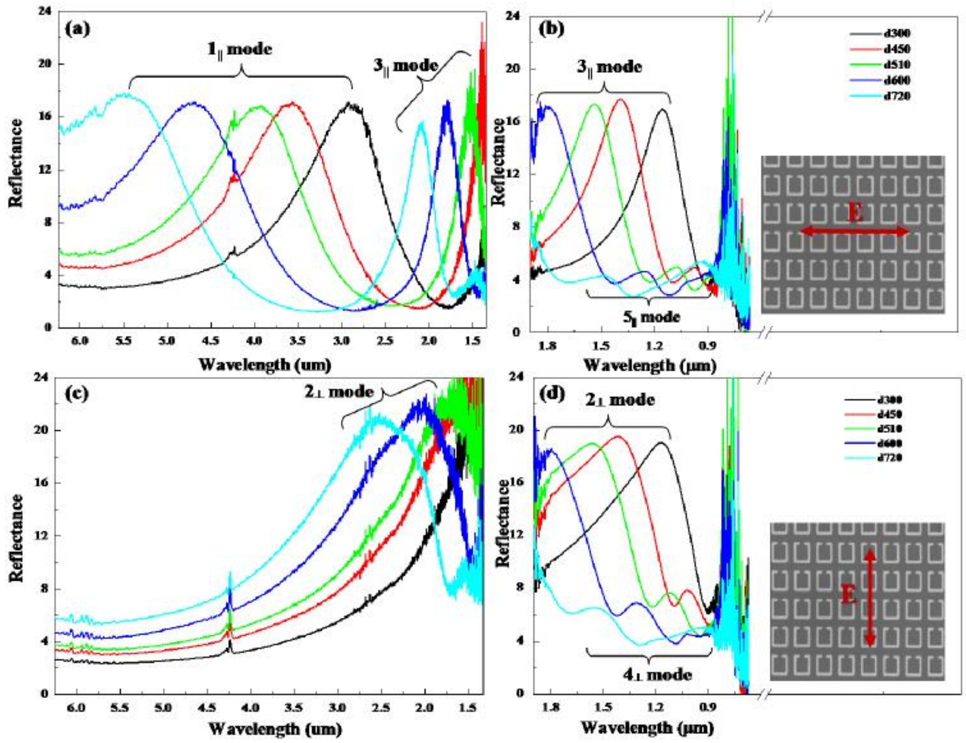

Fig. 2. (a)-(d) The normalized reflectance spectra of five different sized planar SRRs. The left panel is measured within the mid infrared (MIR) region and the right panel is measured within the near infrared (NIR) by μ-FTIR. In near infrared (NIR) measurement, the cut off at 0.8μm is due to instrument limit.

#125448 - $15.00 USD Received 19 Mar 2010; revised 14 Apr 2010; accepted 14 Apr 2010; published 22 Apr 2010

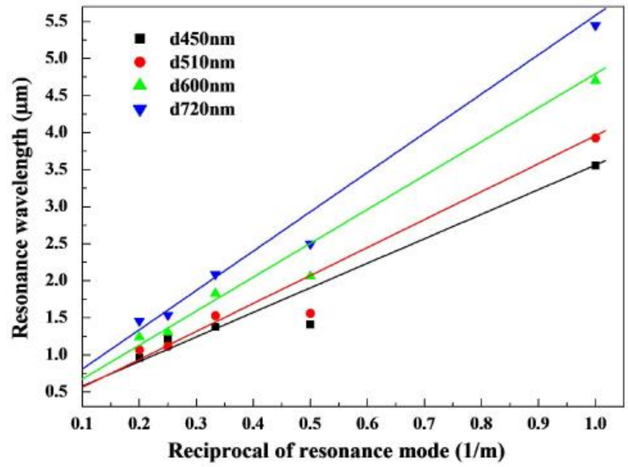

Fig. 3. Resonance wavelength (λ_m) versus the reciprocal of resonance mode (1/m). All curves show a clear linear relationship. Among four samples, the longer SRR displays a greater slope, which is consistent with the SWPR model.

In accordance with the SWPR model, it is possible to predict the sensitivity of SRR-based refractive-index (RI) sensors. In Eq. (1), the effective refractive index of dielectric environment, n_{eff}, stems from the collective contribution of substrates (n_{sub}), analytes (n_a) and surroundings (n_{sur}) and we assume and a linear combination among them so that n_{eff} is expressed as below,

$$n_{eff} = \sum_{i=1}^{k} x_i n_i = x_{sub} n_{sub} + x_a n_a + (1 - x_{sub} - x_a) n_{air} \tag{2}$$

where x_i and n_i represent the fraction and the refractive index of the species *i*, respectively. While varying the analyte on the SRR plasmonic sensor, we introduce a fluctuation of the effective refractive index, d_{neff}, leading to a wavelength shift in reflectance peaks $d\lambda_m$. Thus, the corresponding sensitivity of the SRR sensor turns to be,

$$S\,(sensitivity) = \frac{\partial \lambda_m}{\partial n_a} = \frac{\partial \lambda_m}{\partial n_{eff}} \cdot \frac{\partial n_{eff}}{\partial n_a} = \frac{2L}{m} \cdot \frac{\partial n_{eff}}{\partial n_a} - \frac{\partial \lambda_o}{\partial n_a} = x_a \cdot \frac{2L}{m} - \frac{\partial \lambda_o}{\partial n_a} \tag{3}$$

For such a scalable, coupler-free, and multi-mode refractive index (MMRI) sensor, this derived model clearly provides a quantitative description of the sensitivity (S) with respect to the resonance mode (m) and the size of the SRR structure (L), whose linear relationship indicates that the SRR structure promises an excellent RI sensor for practical applications [26].

Next, we apply a thin layer of PMMA on top of the planar SRRs and measure the reflectance spectra of multiple resonance modes to examine this sensitivity formula. All five different sized planar SRRs respond a significant red shift in multi-mode reflectance peaks and the sensing spectrum of d510 sample is represented in Fig. 4. Notice that a couple of resonance peaks cannot be collected in our measurements; for example, the signal of the 1st resonance mode in d600 and d720 were blocked by the inherit absorption of PMMA around 5.8 μm, the resonance frequency of the 5th resonance mode in d300 is beyond the detection limit of the FTIR microscope. A careful design of operation ranges can keep this SRR plasmonic sensor away from the frequency of the absorption from analytes and the cut-off from the spectrometer. Based on the wavelength shifts within different resonance modes, sensitivity of SRR plasmonic sensor can be calculated. As shown in Fig. 5, the sensitivity linearly depends on the reciprocal of resonance modes, and shows a maximal in the primary resonance mode as Eq. (3) predicted. Moreover, by comparing the sensitivity behavior

#125448 - $15.00 USD Received 19 Mar 2010; revised 14 Apr 2010; accepted 14 Apr 2010; published 22 Apr 2010

between two samples d450 and d510, the latter owns higher sensitivity due to its longer resonance wavelength and indicates an excellent value of 2700 nm/RIU at the 1st resonance. This result further indicates superior sensitivity (i.e. higher than 2700 nm/RIU) can be achieved by simply enlarging the size of SRR, according to the quantitative model.

Comparing with other RI biosensors, the SRR plasmonic biosensor possesses comparable or even better performance, for example, the sensitivity of prism coupler-based surface plasmon polariton (SPP) biosensors in wavelength interrogation ranges from 970 to 13800 nm/RIU, depending on the resonance wavelength [1]; besides, the sensitivity of localized surface plasmon resonance (LSPR) biosensors is from 120 nm/RIU [27] to 500 nm/RIU [28]. It's worthy to notice that the sensitivity of the SRR sensors can be further enhanced based on our proposed model, for example, choosing a substrate of a small refractive index (in accordance with Eq. (2)) and enlarging the size of the SRR structures (in accordance with Eq. (3)).

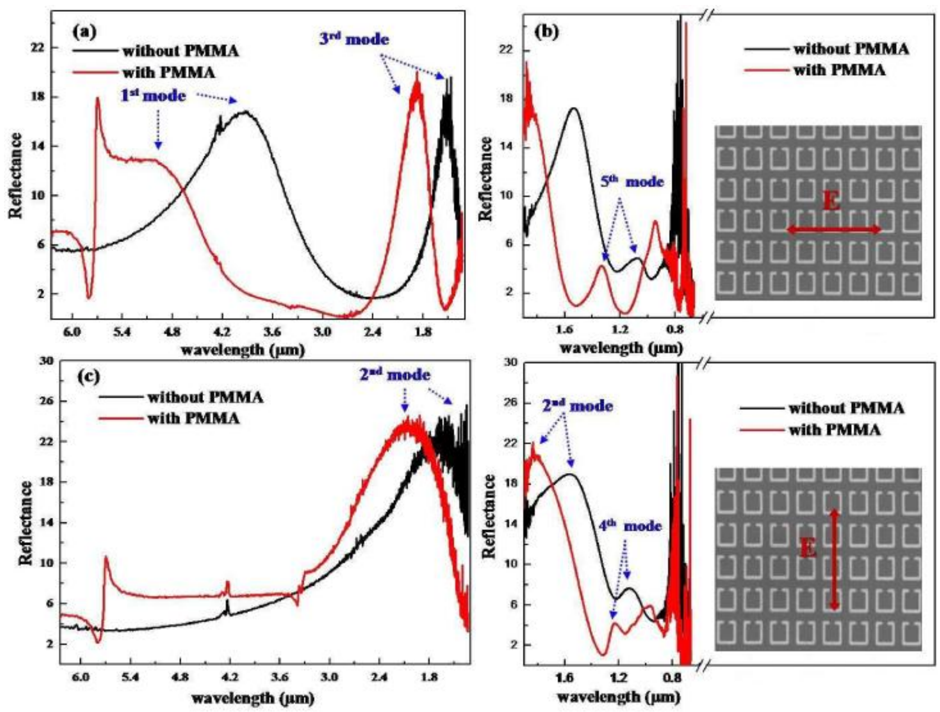

Fig. 4. (a)-(d) Normalized reflectance spectrum of d510 planar SRRs. The left panel is measured within the mid infrared (MIR) region and the right panel is measured within the near infrared (NIR) by μ-FTIR. Red and black curves represent the responses with and without a layer of PMMA film.

#125448 - $15.00 USD Received 19 Mar 2010; revised 14 Apr 2010; accepted 14 Apr 2010; published 22 Apr 2010

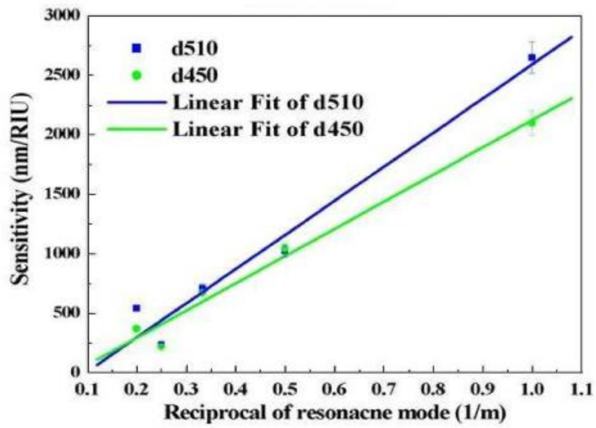

Fig. 5. Linear relationship between resonance wavelength (λ_m) and the reciprocal of resonance mode (1/m). The slope is proportional to total length of SRR (L) and correction factor (x_a).

In addition to quantitatively demonstrating the sensitivity of the SRR plasmonic biosensor, we also investigate its detection length by gradually increasing the thickness of the applied dielectric layer (PMMA) atop until the corresponding wavelength shift saturated. Simulation result of d600 nm is presented in Fig. 6(a). For lower resonance modes $1_{\parallel}$, $2\perp$ and $3_{\parallel}$ resonance modes, the shift of wavelength saturates as the thickness of PMMA layers is about 200 nm to 500 nm; in contrast, for higher resonance modes $4\perp$ and $5_{\parallel}$ resonance modes, no saturation effect is observed even as the thickness rises to 2 μm (see in Fig. 6(b)), a much farther detection length beyond conventional SPR sensors' capability [2]. In fact, for all sizes of SRRs sensors regardless of their resonance frequencies, $1_{\parallel}$, $2\perp$ and $3_{\parallel}$ modes always saturate quickly as the thickness is less than 500 nm whereas $4\perp$ and $5_{\parallel}$ resonance modes still shift even the thickness is up to 2 μm. The detection length of SRR plasmonic biosensors significantly depends upon the resonance mode, due to the localization of electric field (E-field). For lower-order modes, a greater portion of the E-field is strongly localized at the interface between the SRR structure and the overlaid dielectric layer, resulting in shorter detection distance but greater sensitivity; on the other hand, for higher-order modes the penetration depth extends to farther than 2 μm with less sensitivity.

#125448 - $15.00 USD Received 19 Mar 2010; revised 14 Apr 2010; accepted 14 Apr 2010; published 22 Apr 2010

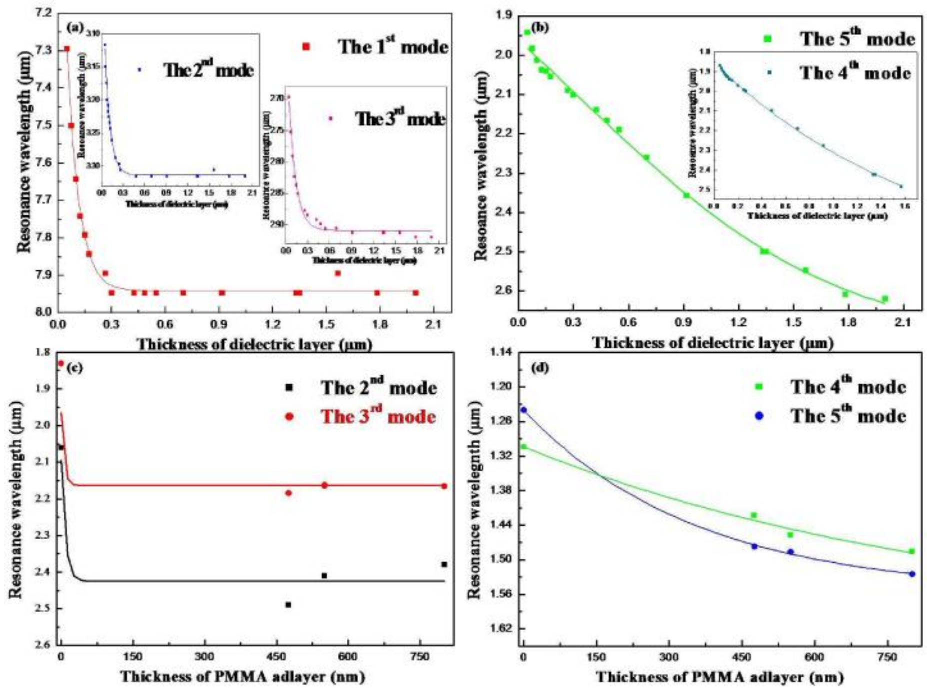

Fig. 6. (a)(b) Simulated results of the varied detection lengths with respect to 1st to 5th resonance modes (for the sample d600). (c) Measured thickness effect of 2nd and 3rd resonance modes. (d) Measured thickness effect of left 4th and 5th resonance modes.

Experimental verification agrees well with the simulation result as shown in Fig. 6(c) and (d). Due to weaker signals limited by the absorption in thicker adlayers, here the thickest PMMA we spun on is around 900 nm. The measurement result shows that the lower modes (i.e., 2^{nd} and 3^{rd} modes in Fig. 6(c)) saturate within 450 nm but the higher modes (i.e., 4^{th} and 5^{th} modes in Fig. 6(d)) do not even the thickness is beyond 900 nm. As a result, for biosensing applications the lower modes can be utilized to detect small targets and macro molecules including antibody-antigen interactions and the molecular recognition on the cell membrane, to gain the advantage of the excellent sensitivity and also to reduce noise from the dielectric environment; the higher modes facilitate to explore intracellular bio-events in live organelles and cells, due to their farther detection lengths in micron scale as well as label-free manner. Such a multi-functional plasmonic biosensor can be readily employed for the analysis of activation-dependent cellular interactions and even a potential label-free bio-imaging device that other label-free techniques have not been achieved.

In conclusion, we investigated the sensing performance of a multi-functional SRR-based plasmonic sensor, including its sensitivity and detection lengths with respect to multiple resonance modes. Deduced from the standing-wave plasmonic resonance model, we manifested a quantitative formula among the sensitivity, resonant modes and the size of SRR nano-structures, verified by both simulation and experiments. In addition to sensitivity, the dependency between detection lengths and resonance modes was also clarified. In short, the lower resonance modes exhibit excellent sensitivity with shorter detection lengths to target small and macro molecules; the higher resonance modes can be employed to explore intracellular bio-events in live organelles and cells. Our study has provided a clear designing guideline for SRR-based multi-functional plasmonic sensor. By collecting signals from these modes, such a plasmonic sensor provides a solution for different sensing purposes, and possesses further advantages beyond other optical sensors such as label-free and real-time diagnosis (vs. fluorescent and Raman scattering techniques), coupler free to avoid the issues of coupling oil leakage and dispersion, great detection lengths (vs. SPP techniques), and

#125448 - $15.00 USD Received 19 Mar 2010; revised 14 Apr 2010; accepted 14 Apr 2010; published 22 Apr 2010

scalable operation frequencies (vs. LSPR techniques) in particular in IR regimes to prevent strong absorption from bio-agents, serving as a multi-functional biosensor and even a potential bio-imaging device for live cells.

Acknowledgments

The authors gratefully acknowledge the financial support from National Science Council (NSC 95-2112-M-007 –048 MY3), Chang Gung Memorial Hospital (CGMH 99N2432E1) and Ministry of Economic Affairs (97-EC-17-A-08-S1-03) for this study.

#125448 - $15.00 USD   Received 19 Mar 2010; revised 14 Apr 2010; accepted 14 Apr 2010; published 22 Apr 2010